MACHINE-TOOL SETTINGS TO PROVIDE OPTIMAL TCA OF SPIRAL BEVEL GEAR DRIVES

Mohammad Qasim Abdullah
Assist. Prof. in Mechanical Engineering Department
College of Engineering / University of Baghdad

ABSTRACT

The present paper presents an approach to optimize tooth contact analysis (TCA) of spiral bevel gear drivin by controlling the machine-tool settings that directly affects the shape of tooth and behavior of meshing and contact for mating gears. The proposed settings provide a pre-designed parabolic function of transmission errors and the desired location and orientation of the bearing contact. The main goal of detecting the pre-designed parabolic function of transmission errors is to reduce the gear noise which can be done by absorbing the linear function of transmission errors that are caused by gear misalignment. The model is generated with means of CAD software package and solid works program, the basic input design data imported by Gleason works standards.

الخلاصة:

في هذا البحث تم تقديم وسيلة لإيجاد أفضل تحليل لتلامس الأسنان للمسنن المخروطي الحلزوني وذلك بواسطة التحكم بضبط موقع الأداة لماكنة القطع الخاصة بهذا النوع من المسننات والتي تؤثر بشكل مباشر على شكل السن وسلوك المحاكاة والتلامس بين المسننات المتعاشقة. إن الضبط المقترح لأداة القطع سوف يأخذ بنظر الاعتبار الأخطاء المتولدة من جراء آلية نقل الحركة وكذلك موقع التحميل ومنحى التلامس الحاصل بين الأسنان. إن الهدف الرئيسي من هذا البحث هو تقليل الخطأ الحاصل من جراء آلية نقل الحركة والمتسبب من عدم التطابق بين المسننات المتعاشقة، وذلك لتخفيض مستوى الضوضاء المتولدة منها عند التعشيق. ولغرض الشروع في هذه الدراسة، تم استخدام برنامج جاهز لتوليد النماذج الخاصة بهذا النوع من المسننات وفقاً لبيانات إدخال قياسية استخدمت لهذا الغرض.

KEYWORDS: Gear, Spiral, Bevel, Tool, Setting, TCA.

INTRODUCTION

Tooth Contact Analysis (TCA) is a computational approach for analyzing the nature and quality of the meshing contact in a pair of gears. The concept of TCA was originally introduced in early 1960s as a research tool, and applied to spiral bevel gears. It is a powerful tool for the design and analysis of spiral bevel gear drives. Typical outputs of TCA are the graphs of contact patterns and transmission errors.

TCA can simulate gear meshing contact characteristics under light and heavy loads. TCA program have been widely employed by gear engineers and researchers in their design of high strength and low noise spiral bevel gear drives.

Application of TCA technology resulted in significant improvement in the development of bevel gear pairs, under given contact conditions **(Lelkes and Marialigeti , 2002).**

Basically, machine tool setting means the guide to design and manufacture the gear drive. In the present work, a developed approach has been proposed to control and design suc a gear drive by simulating the meshing and changing the machine-tool settings to get optimal TCA.

There are two methods for manufacturing spiral bevel gears, face milling and face hobbing. Both of which are widely employed by the gear manufacturing industry and can be implemented on modern CNC bevel gear generators **(Litvin and Lee , 1989).**

Fig.(1) shows a 3D geometric model of spiral bevel gear.

MACHINE-TOOL SETTENGS AND TCA

Gear Machine-Tool Settings

The proposed design provides the following:

The gear-generating surface by $\sum_G$, the generated gear surface by $\sum_2$, the pinion-generating tool surface by $\sum_P$, and the generated pinion surface $\sum_1$.

To set up the gear machine-tool settings, the following data should be given:

Γ: shaft angle
N_2: gear tooth number, N_1: pinion tooth number
γ_2: gear root angle
A: mean pitch cone distance
β: mean spiral angle
ψ_G: blade angle for gear cutter
d_G: average diameter of gear cutter
w_G: point width

The gear pitch angle is represented by (Faydor L. Litvin and Alfonso Fuentes, 2004):

$$\mu_2 = \arctan \frac{\sin \Gamma}{\frac{N_1}{N_2} + \cos \Gamma} \quad (1)$$

The pinion pitch angle is:

$$\mu_1 = \Gamma - \mu_2 \quad (2)$$

The dedendum angles are:

$$\delta_1 = \mu_1 - \gamma_1 \text{ and } \delta_2 = \mu_2 - \gamma_2 \quad (3)$$

Gear Cutting Ratio

The process of gear generation is based on the imaginary meshing of a crown-gear with the member-gear **(Qi Fan 2006).**

The instantaneous axis of rotation by such meshing coincides with the pitch line axis Z_P, as shown in **Figs. (3)** and **(4).**

The generating surface $\sum_G$ which may be imagined as the surface of the crown gear, and be generated gear surface $\sum_2$ contact each other at a line at every instant. The ratio of angular velocities of the crown gear and the being generated gear (the cutting ratio) remains constant while the spatial line of contact moves over surfaces $\sum_G$ and $\sum_2$.

The gear cutting ratio can be represented as follows **(Litvin and Lee 1989):**

$$m_{G2} = \frac{\omega^{(G)}}{\omega^{(2)}} = \frac{\sin \mu_2}{\cos \delta_2} \quad (4)$$

Cutter Tip Radius, Radial Setting, and Cradle Angle

From **Fig.(5)**, it can be obtained the inside and outside tip radii of the head-cutter as follows **(Litvin and Lee 1989):**

$$r_G = \frac{1}{2}(d_G \mp w_G) \quad (5)$$

Also, from the relation between the lengths and angles of the triangle $O_m O_c M_G$ of the same figure, it can be expressed the radial setting S_G and cradle angle q_G as follows:

$$S_G = \sqrt{\frac{d^2}{4} + A^2 \cos^2 \delta_2 - d_G A \cos \delta_2 \sin \beta} \quad (6)$$

and

$$q_G = \arccos \frac{A^2 \cos^2 \delta_2 + S_G^2 - d_G^2 / 4}{2 A S_G \cos \delta_2} \quad (7)$$

DETERMINATION ANALYSIS OF THE MEAN CONTACT POINT

The gear and pinion surfaces of spiral bevel gears are in point contact at every instant. The mean contact point is the center of the bearing contact and its location is selected generally at the middle of the working depth on gear tooth. **Fig.(6)** shows a gear tooth surface. Section AD is the gear tip, section BC is the pinion tip and it is parallel to the root line of the gear, and the working area is within ABCD **(Faydor and Alfonso 2003).**

The mean contact point is located on a line which passes through the middle point of the two points at which the normal section of the gear surface intersects line AD and line BC respectively. In addition, the mean contact point must be on the gear surface. This means that is must satisfy the equation of meshing for the gear being generated by the tool. From these two requirements, the location of the mean contact point is determined **(Joseph and Thomas 2003).**

RELATION BEWEEN DIRECTIONS OF THE PATHS OF THE MEAN CONTACT POINT OVER THE GEAR AND PINION TOOTH SURFACES

Fig.(7) shows the tangent plane to the gear and pinion surface at the mean contact point B. The relation between angles υ_1 and υ_2 depends on parameters in motion and the principal curvatures of the gear tooth surface.

This relation can be expressed as follow (Gosselin C, Cloutier L and Brousseau J., 1991):

$$\tan\upsilon_1 = \frac{(a_{33} + a_{31}V_{2I}^{(12)})\tan\upsilon_2 - a_{31}V_{2II}^{(12)}}{a_{32}(V_{2II}^{(12)} - V_{2I}^{(12)}\tan\upsilon_2) + a_{33}} \qquad (8)$$

PINION MACHINE – TOOL SETTINGS

There are five machine-tool settings m_{p1}, E_m, L_m, s_p, and q_p to be determined. The key to the solution of this problem is the determination of the cutting ratio m_{p1} (Lelkes M. and Marialigeti J., 2002).

Determination of Pinion Cutting Ratio

Consider that surfaces $\sum_1$ and $\sum_F$ are equivalent, and that surfaces $\sum_p$ and $\sum_Q$ are equivalent.

Also the following data must be given **(Lelkes and Marialigeti 2002):**

1- The principal curvatures of the pinion surface at the mean contact point, k_{1I} and k_{1II}.
2- The principal directions of the pinion surface at the mean contact point, $\vec{e}_{1I}$ and $\vec{e}_{1II}$.
3- The coordinates of the mean contact point.
4- The unit normal at the mean contact point.
5- The coefficients a_{11}, a_{12}, and a_{22}.

The procedure to determine m_{p1} is as follows **(Robert Handschuh 1997):**

Step 1: The angular velocity of the pinion is represented by

$$\vec{\omega}^{(1)} = \pm\begin{bmatrix} \sin\mu_1 \\ 0 \\ \cos\mu_1 \end{bmatrix} \tag{9}$$

The angular velocity of the pinion cutter is represented by:

$$\vec{\omega}^{(p)} = \pm m_{p1}\omega^{(1)}\begin{bmatrix} \cos\delta_1 \\ 0 \\ -\sin\delta_1 \end{bmatrix} \tag{10}$$

Therefore, the relative angular velocity $\vec{\omega}^{(1p)}$ can be obtained as follows:

$$\vec{\omega}^{(1p)} = \pm\omega^{(1)}\begin{bmatrix} \sin\mu_1 - m_{p1}\cos\delta_1 \\ 0 \\ \cos\mu_1 + m_{p1}\sin\delta_1 \end{bmatrix} \tag{11}$$

Step 2: Representation of $\left[\vec{\omega}^{(1p)}\vec{n}\vec{e}_{pI}\right]$

The scalar $\left[\vec{\omega}^{(1p)}\vec{n}\vec{e}_{pI}\right]$ is represented by:

$$\left[\vec{\omega}^{(1p)}\vec{n}\vec{e}_{pI}\right] = \omega^{(1)}\begin{vmatrix} \pm(\sin\mu_1 - m_{p1}\cos\delta_1) & 0 & \pm(\cos\mu_1 + m_{p1}\sin\delta_1) \\ n_x & n_y & n_z \\ e_{PIx} & e_{PIy} & e_{PIz} \end{vmatrix}$$

$$= \begin{Bmatrix} \left[(n_z e_{PIy} - n_y e_{PIz})\cos\delta_1 + (n_x e_{PIy} - n_y e_{PIx})\sin\delta_1\right]m_{p1} \\ +\left[(n_y e_{PIx} - n_z e_{PIy})\sin\mu_1 + (n_x e_{PIy} - n_y e_{PIx})\cos\mu_1\right] \end{Bmatrix}\omega^{(1)}$$

$$= (C_{11}m_{p1} + C_{12})\omega^{(1)} \tag{12}$$

Step 3: Representation of $\left[\vec{\omega}^{(1p)}\vec{n}\vec{e}_{PII}\right]$

The scalar $\left[\vec{\omega}^{(1p)}\vec{n}\vec{e}_{PII}\right]$ is represented by:

$$\left[\vec{\omega}^{(1p)}\vec{n}\vec{e}_{PII}\right] = \omega^{(1)}\begin{vmatrix} \pm(\sin\mu_1 - m_{p1}\cos\delta_1) & 0 & \pm(\cos\mu_1 + m_{p1}\sin\delta_1) \\ n_x & n_y & n_z \\ e_{PIIx} & e_{PIIy} & e_{PIIz} \end{vmatrix}$$

$$= \pm\left[(n_y e_{PIIz} - n_z e_{PIIy})\sin\mu_1 + (n_x e_{PIIy} - n_y e_{PIIx})\cos\mu_1\right]\omega^{(1)}$$

$$= C_{22}\omega^{(1)} \tag{13}$$

Step 4: Representation of $\vec{V}^{(1p)}$

The velocity $\vec{V}^{(1)}$ may be obtained by:

$$\vec{V}^{(1)} = \vec{\omega}^{(1)} x \vec{B}$$

$$= \pm\omega^{(1)} \begin{bmatrix} -B_y \cos\mu_1 \\ B_x \cos\mu_1 - B_Z \sin\mu_1 \\ B_y \sin\mu_1 \end{bmatrix} \quad (14)$$

The velocity $\vec{V}^{(p)}$ may be obtained by:

$$\vec{V}^{(p)} = \vec{\omega}^{(p)} x \vec{B} + \overline{O_f O_m} x \vec{\omega}^{(p)}$$

$$= \omega^{(1)} m_{p1} \begin{bmatrix} (E_m \pm B_y)\sin\delta_1 \\ \pm(L_m - B_x \sin\delta_1 - B_y \cos\delta_1 \\ (E_m \pm B_y)\cos\delta_1 \end{bmatrix} \quad (15)$$

So, the sliding velocity $\vec{V}^{(1p)}$ is described by:

$$\vec{V}^{(1p)} = \vec{V}^{(1)} - \vec{V}^{(p)}$$

$$= \omega^{(1)} \begin{bmatrix} \pm B_y \cos\mu_1 - m_{p1}(E_m \pm B_y)\sin\delta_1 \\ \pm(B_x \cos\mu_1 - B_z \sin\mu_1) \pm m_{p1}[L_m - (B_x \sin\delta_1 + B_z \cos\delta_1)] \\ \pm B_y \sin\mu_1 - m_{p1}(E_m \pm B_y)\cos\delta_1 \end{bmatrix} \quad (16)$$

Step 5: Representation of $V_{PI}^{(1p)}$ and $V_{PII}^{(1p)}$

$$a_{13} = -k_{PI} V_{PI}^{(1p)} - (C_{11} m_{p1} + C_{12})\omega^{(1)} \quad (17)$$

$$a_{23} = -k_{PII} V_{PII}^{(1p)} - C_{22}\omega^{(1)} \quad (18)$$

$$a_{11} a_{23} - a_{12} a_{13} = 0 \quad (19)$$

By using **Eqs. (17), (18),** and **(19):**

$$a_{12} k_{PI} V_{PI}^{(1p)} - a_{11} k_{PII} V_{PII}^{(1p)} = \left[-a_{12} C_{11} m_{p1} + (a_{11} C_{22} - a_{12} C_{12})\right]\omega^{(1)} \quad (20)$$

Also, it can be deduced that:

$$\vec{V}^{(1p)} = V_{PI}^{(1p)} \vec{e}_{PI} + V_{PII}^{(1p)} \vec{e}_{PII} \quad (21)$$

By considering only the x component in **Eqs. (16)** and **(21):**

$$V_{PI}^{(1p)} e_{PIx} + V_{PII}^{(1p)} e_{PIIx} = [\pm B_y \cos\mu_1 - m_{p1}(E_m \pm B_y)\sin\delta_1]\omega^{(1)} \quad (22)$$

Also by considering only the z component in **Eqs. (16)** and **(21):**

$$V_{PI}^{(1p)} e_{PIz} + V_{PII}^{(1p)} e_{PIIz} = [\pm B_y \sin\mu_1 - m_{p1}(E_m \pm B_y)\cos\delta_1]\omega^{(1)} \quad (23)$$

By multiplying **Eq. (22)** by cosδ1 and **Eq. (23)** by sinδ1, and adding the resulting equations:

$$V_{PII}^{(1p)} = \pm \frac{B_y \cos\gamma_1}{e_{PIIx}\cos\delta_1 - e_{PIIz}\sin\delta_1}\omega^{(1)} = t_1\omega^{(1)} \tag{24}$$

Then, substituting **Eq.(24)** into **Eq.(22):**

$$V_{PI}^{(1p)} = (-\frac{C_{11}}{k_{PI}}m_{p1} + \frac{a_{11}k_{PII}t_1 + a_{11}C_{22} - a_{12}C_{12}}{a_{12}k_{PI}})\omega^{(1)}$$

$$= (t_1 m_{p1} + t_2)\omega^{(1)} \tag{25}$$

Step 6: Representation of $\vec{V}^{(1p)}$

The matrix form of **Eq.(21)** may be represented by:

$$\vec{V}^{(1p)} = \begin{bmatrix} V_{PI}^{(1p)}e_{PIx} + V_{PII}^{(1p)}e_{PIIx} \\ V_{PI}^{(1p)}e_{PIy} + V_{PII}^{(1p)}e_{PIIy} \\ V_{PI}^{(1p)}e_{PIz} + V_{PII}^{(1p)}e_{PIIz} \end{bmatrix} \tag{26}$$

By substituting **Eqs. (24)** and **(25)** into **Eq.(26):**

$$\vec{V}^{(1p)} = \omega^{(1)}\begin{bmatrix} (t_1 m_{p1} + t_2)e_{PIx} + t_4 e_{PIIx} \\ (t_1 m_{p1} + t_2)e_{PIy} + t_4 e_{PIIy} \\ (t_1 m_{p1} + t_2)e_{PIz} + t_4 e_{PIIz} \end{bmatrix}$$

$$= \omega^{(1)}\begin{bmatrix} u_{11}m_{p1} + u_{12} \\ u_{21}m_{p1} + u_{22} \\ u_{31}m_{p1} + u_{32} \end{bmatrix} \tag{27}$$

Step 7: Representation of $\left[\vec{n}\vec{\omega}^{(1p)}\vec{V}^{(1p)}\right]$

The scalar $\left[\vec{n}\vec{\omega}^{(1p)}\vec{V}^{(1p)}\right]$ may by represented by:

$$\left[\vec{n}\vec{\omega}^{(1p)}\vec{V}^{(1p)}\right] = [\omega^{(1)}]^2 \begin{vmatrix} n_x & n_y & n_z \\ \pm(\sin\mu_1 + m_{p1}\cos\delta_1) & 0 & \pm(\cos\mu_1 + m_{p1}\sin\delta_1) \\ u_{11}m_{p1} + u_{12} & u_{21}m_{p1} + u_{22} & u_{31}m_{p1} + u_{32} \end{vmatrix}$$

$$= (\upsilon_1 m_{p1} + \upsilon_2 m_{p1} + \upsilon_3)[\omega^{(1)}]^2 \tag{28}$$

Where:

$$\upsilon_1 = \pm\left[(u_{11}\sin\delta_1 - u_{31}\cos\delta_1)n_y - (n_z\cos\delta_1 + n_x\sin\delta_1)u_{21}\right] \tag{29}$$

$$\upsilon_2 = \mp\begin{bmatrix} (u_{21}\cos\mu_1 + u_{22}\sin\delta_1)n_x - (u_{21}\sin\mu_1 - u_{22}\cos\delta_1)n_z \\ -(u_{11}\cos\mu_1 + u_{12}\sin\delta_1 + u_{32}\cos\delta_1 - u_{31}\sin\mu_1)n_y \end{bmatrix} \tag{30}$$

$$\upsilon_3 = \mp\left[(u_{22}n_x\cos\mu_1) - (u_{12}\cos\mu_1 - u_{32}\sin\mu_1)n_y - u_{22}n_z\sin\mu_1\right] \tag{31}$$

Step 8: Representation of $\vec{n}.(\vec{\omega}^{(1)}x\vec{V}^{(p)} - \vec{\omega}^{(p)}x\vec{V}^{(1)})$

The velocity $\vec{V}^{(p)}$ may be described by:

$$\vec{V}^{(p)} = \vec{V}^{(1)} - \vec{V}^{(1p)} \tag{32}$$

Now, substituting **Eqs.(14)** and **(27)** into **Eq.(32):**

$$\vec{V}^{(p)} = \omega^{(1)}\begin{bmatrix} -u_{11}m_{p1} \mp B_y\cos\mu_1 - u_{12} \\ -u_{21}m_{p1} \mp B_z\sin\mu_1 \pm B_x\cos\mu_1 - u_{22} \\ -u_{31}m_{p1} \pm B_y\sin\mu_1 - u_{32} \end{bmatrix} \tag{33}$$

Vector $(\vec{\omega}^{(1)}x\vec{V}^{(p)})$ is represented by:

$$\vec{\omega}^{(1)}x\vec{V}^{(p)} = [\omega^{(1)}]^2\begin{bmatrix} \pm[u_{21}m_{p1} - (B_z\sin\mu_1 - B_x\cos\mu_1 \pm u_{22})]\cos\mu_1 \\ (\mp u_{11}\cos\mu_1 \pm u_{31}\sin\mu_1)m_{p1} - B_y \pm u_{12}\cos\mu_1 \pm u_{32}\sin\mu_1 \\ \mp[u_{21}m_{p1} - (B_z\sin\mu_1 - B_x\cos\mu_1 \pm u_{22})]\sin\mu_1 \end{bmatrix} \tag{34}$$

Vector $(\vec{\omega}^{(p)}x\vec{V}^{(1)})$ is represented by:

$$(\vec{\omega}^{(p)}x\vec{V}^{(1)}) = [\omega^{(1)}]^2\begin{bmatrix} -(B_z\sin\mu_1 - B_x\cos\mu_1)m_{p1}\sin\delta_1 \\ -B_y m_{p1}\sin\gamma_1 \\ -(B_z\sin\mu_1 - B_x\cos\mu_1)m_{p1}\cos\delta_1 \end{bmatrix} \tag{35}$$

Subtracting **Eq.(35)** from **Eq.(34):**

$$\vec{\omega}^{(1)}x\vec{V}^{(p)} - \vec{\omega}^{(p)}x\vec{V}^{(1)} = [\omega^{(1)}]^2\begin{bmatrix} h_{11}m_{p1} + h_{12} \\ h_{21}m_{p1} + h_{22} \\ h_{31}m_{p1} + h_{32} \end{bmatrix} \tag{36}$$

Where:

$$h_{11} = \pm u_{21}\cos\mu_1 - (B_x\cos\mu_1 - B_z\sin\mu_1)\sin\delta_1 \tag{37}$$

$$h_{12} = (B_z\sin\mu_1 - B_x\cos\mu_1 \pm u_{22})\cos\mu_1 \tag{38}$$

$$h_{21} = B_y\sin\gamma_1 \mp u_{11}\cos\mu_1 \pm u_{31}\sin\mu_1 \tag{39}$$

$$h_{22} = -(B_y \pm u_{12}\cos\mu_1 \pm u_{32}\sin\mu_1) \tag{40}$$

$$h_{31} = \mp u_{21}\sin\mu_1 - (B_x\cos\mu_1 - B_z\sin\mu_1)\cos\delta_1 \quad (41)$$

$$h_{32} = -(B_z\sin\mu_1 - B_x\cos\mu_1 \pm u_{22})\sin\mu_1 \quad (42)$$

Therefore, it may be obtained $\vec{n}.(\vec{\omega}^{(1)}x\vec{V}^{(p)} - \vec{\omega}^{(p)}x\vec{V}^{(1)})$ as follows:

$$\vec{n}.(\vec{\omega}^{(1)}x\vec{V}^{(p)} - \vec{\omega}^{(p)}x\vec{V}^{(1)}) = (f_1 m_{p1} + f_2)[\omega^{(1)}]^2 \quad (43)$$

Where:

$$f_1 = n_x h_{11} + n_y h_{21} + n_z h_{31} \quad (44)$$

$$f_2 = n_x h_{12} + n_y h_{22} + n_z h_{32} \quad (45)$$

Step 9: Representation of m_{p1}

Using **Eqs. (12)** and **(25)**, the equation of a_{13} may be represented by:

$$a_{13} = -(k_{PI}t_2 + C_{12})\omega^{(1)} \quad (46)$$

Using Eqs. (11) and (24), a23 may be described by:

$$a_{23} = -(k_{PII}t_4 + C_{22})\omega^{(1)} \quad (47)$$

Using **Eqs. (24), (25),** and **(43)**, the equation for a33 may be represented by:

$$a_{33} = [(2k_{PI}t_1t_2 - \upsilon_2 - f_1)m_{p1} + (k_{PI}t_2^2 + k_{PII}t_4^2 - \upsilon_3 - f_2)][\omega^{(1)}]^2 \quad (48)$$

with:

$$a_{12}a_{33} - a_{13}a_{23} = 0 \quad (49)$$

So, **Eqs. (46), (47), (48),** and **(49)** yield:

$$m_{p1} = -\frac{a_{12}(k_{PI}t_2^2 + k_{PII}t_4^2 - \upsilon_3 - f_2) - (k_{PI}t_2 + C_{12})(k_{PII}t_4 + C_{22})}{a_{12}(2k_{PI}t_1t_2 - \upsilon_2 - f_1)} \quad (50)$$

Determination of Parameters E_m and L_m

Parameters E_m and L_m of the pinion machine-tool settings have been shown in **Figs.(3)** and **(4).** Since the pinion cutting ratio m_{p1} has been determined, it is easy to find these two parameters **(Litvin et.al 2001).**

By using **Eq.(27)** to determine vector $\vec{V}^{(1p)}$ and applying **Eq.(16):**

$$E_m = \frac{\mp B_y\cos\mu_1 - V_x^{(1p)}}{m_{p1}\sin\delta_1} \mp B_y \quad (51)$$

Also:

$$L_m = \frac{B_y \cos\mu_1 - B_z \sin\mu_1 \mp V_y^{(1p)}}{m_{p1}} + B_x \sin\delta_1 + B_z \cos\delta_1 \quad (52)$$

Determination of Pinion Radial Setting and Cradle Angle

The determination of the pinion radial setting and the cradle angle is based on the consideration that the position vectors of the pinion tooth surface and head-cutter must coincide at the mean contact point.

For a straight-edged cutter(Lelkes and Marialigeti 2002)

$$s_p \sin q_p = \pm B_{fy} + E_m \pm u_p \sin\varphi_p \sin\tau_p \quad (53)$$

$$s_p \cos q_p = B_{fx} \sin\delta_1 + B_{fz} \cos\delta_1 - L_m - u_p \sin\varphi_p \cos\tau_p \quad (54)$$

For a curved-edged cutter (Theodore 1981)

$$s_p \sin q_p = \pm B_{fy} + E_m \pm \frac{\cos\tau_p \sin\tau_p}{k_{PI}} \quad (55)$$

$$s_p \cos q_p = B_{fx} \sin\delta_1 + B_{fz} \cos\delta_1 - L_m \pm \frac{\cos\tau_p \cos\tau_p}{k_{PI}} \quad (56)$$

Using $\sin^2 q_p + \cos^2 q_p = 1$, and eliminating q_p then solving for pinion radius s_p. Also eliminating s_p, it can be solved the pinion cradle angle q_p.

NUMERICAL EXAMPLE

The synthesis above is used to determine the machine-tool settings for a pair of spiral bevel gear drive, and then TCA computer program is developed to simulate the meshing of this pair under alignment and misalignment conditions, **Fig.(8)** represent the flow chart of the TCA computer program which has been developed in this work.

The major blank data is represented in **Table (1)**, these data imported from standard Gleason works **(Theodore 1981).**

The straight blade is used to cut the gears and curved blade is used to cut the pinion, and **Table (2)** shows the input design data. **Tables (3)** and **(4)** show the output for the pinion machine-tool settings.

Two conditions of misalignment are considered when the TCA is applied to simulate the meshing. They are the shift of pinion along its axis, which is denoted by ΔA, and the error of pinion shaft offset, which is denoted by ΔV.

The output of TCA program is shown in **Figs. (9 to 18)** and from these figures, its clear that there is a reduction in the transmission error for the case of using curved edged blade, where the value of the transmission error for the case of straight-edged blade with ΔA = − 0.05 mm, [**Fig.(10)**] is about (8 sec.) but for the case of using curved-edged blade with ΔA = − 0.05 mm, [Fig. (16)] is about (7 sec.), i.e. reduction ratio about (12% →15%). Also, the same tendency can be seen when

$\Delta A = +0.05$ mm, [**Fig. (10)** and **Fig. (15)**] and when $\Delta V = -0.05$ mm, [**Fig. (13)** and **Fig. (18)**], or $\Delta V = +0.05$ mm, [**Fig. (12)** and **Fig. (17)**].

CONCLUSION

The main conclusions obtained from present work can be summarized as follows:

1- A developed approach to simulate the optimal meshing and contact of spiral bevel gear drives has successfully applied by controlling the machine-tool settings.
2- A new approach of TCA has been proposed.
3- A computer program to evaluate the pinion machine-tool settings and function of transmission errors has been developed.
4- The results of this computer program show the effect procedure which followed and leads us for controlling the bearing contact by reducing the errors of misalignment.

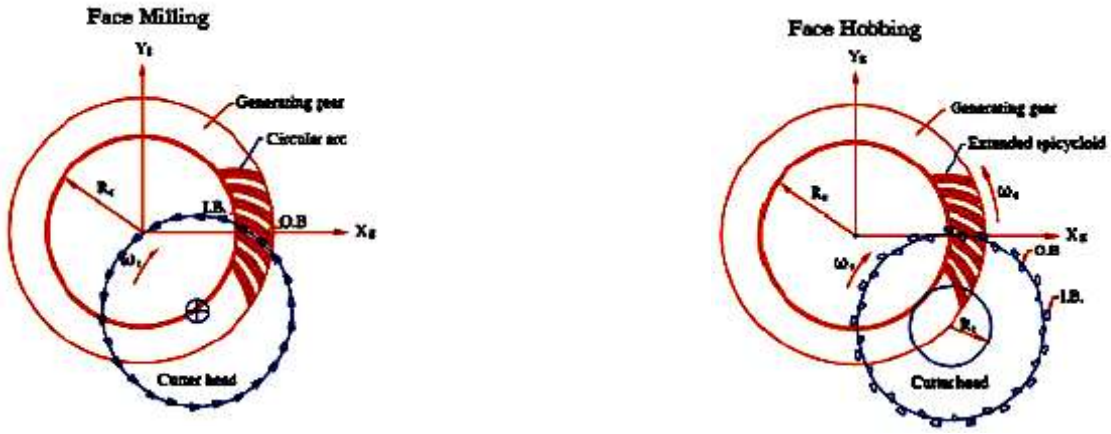

Fig.(1): Face Milling And Face Hobbing Generation Processes

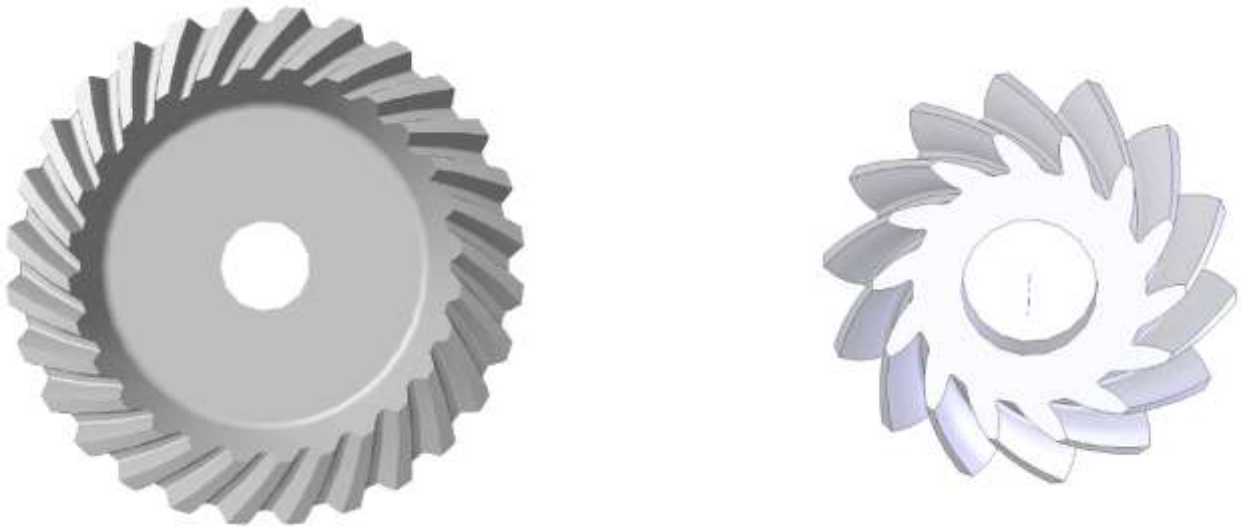

Fig.(2): 3D Geometric Model Of Gear And Pinion Created By Solid Works Program

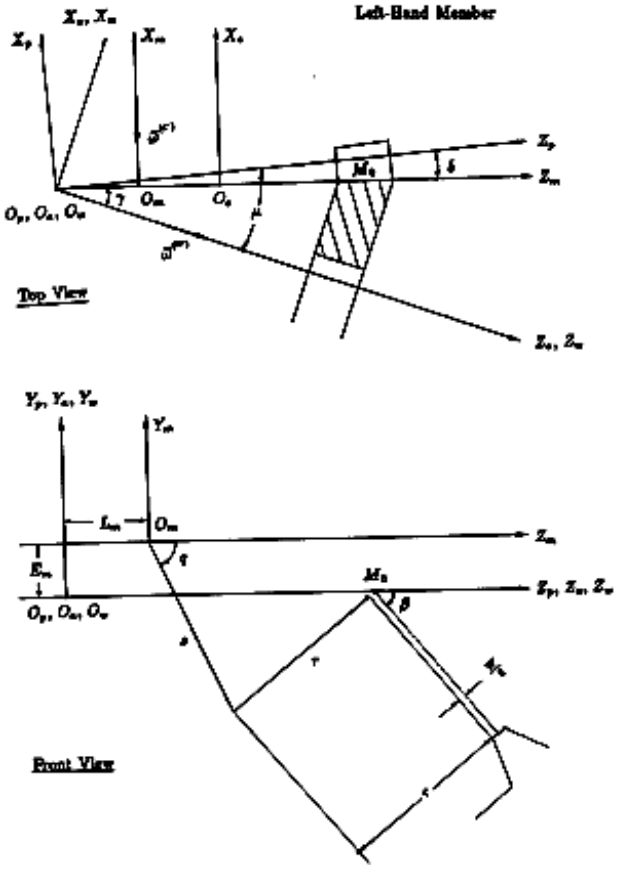

Fig. (3): Top And Front Views Of Left-Hand Gear Generator

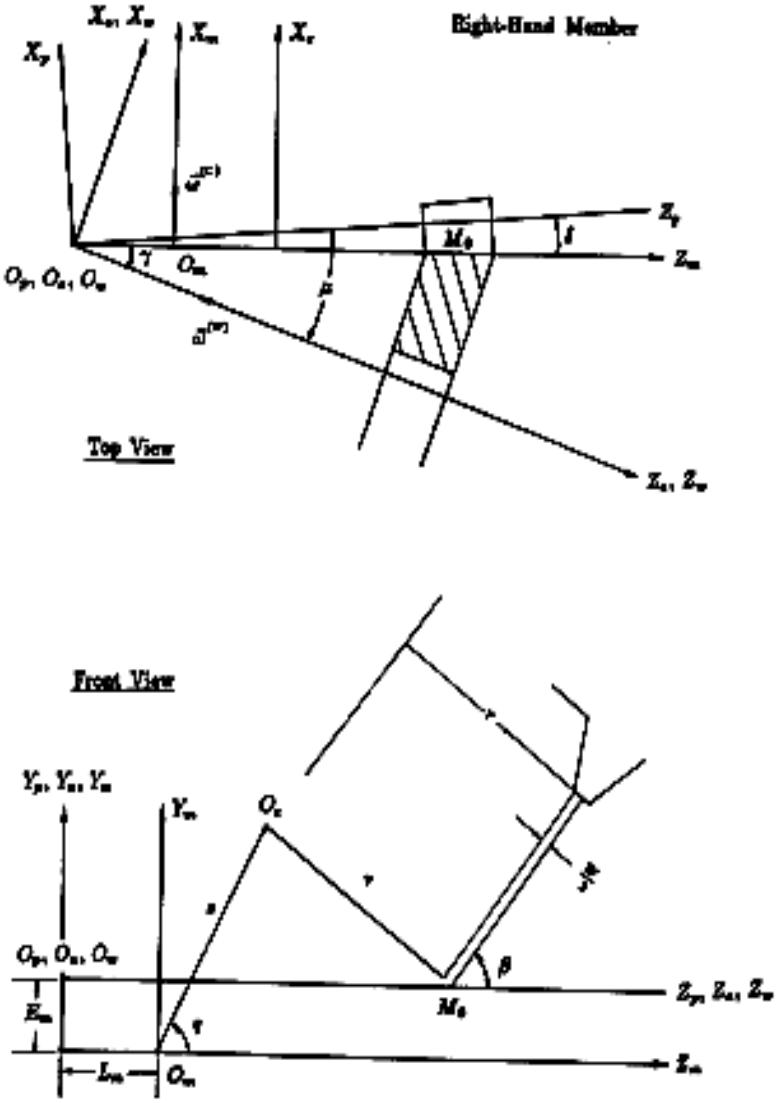

Fig. (4): Top And Front Views Of Right-Hand Gear Generator.

Left-Hand

Right-Hand

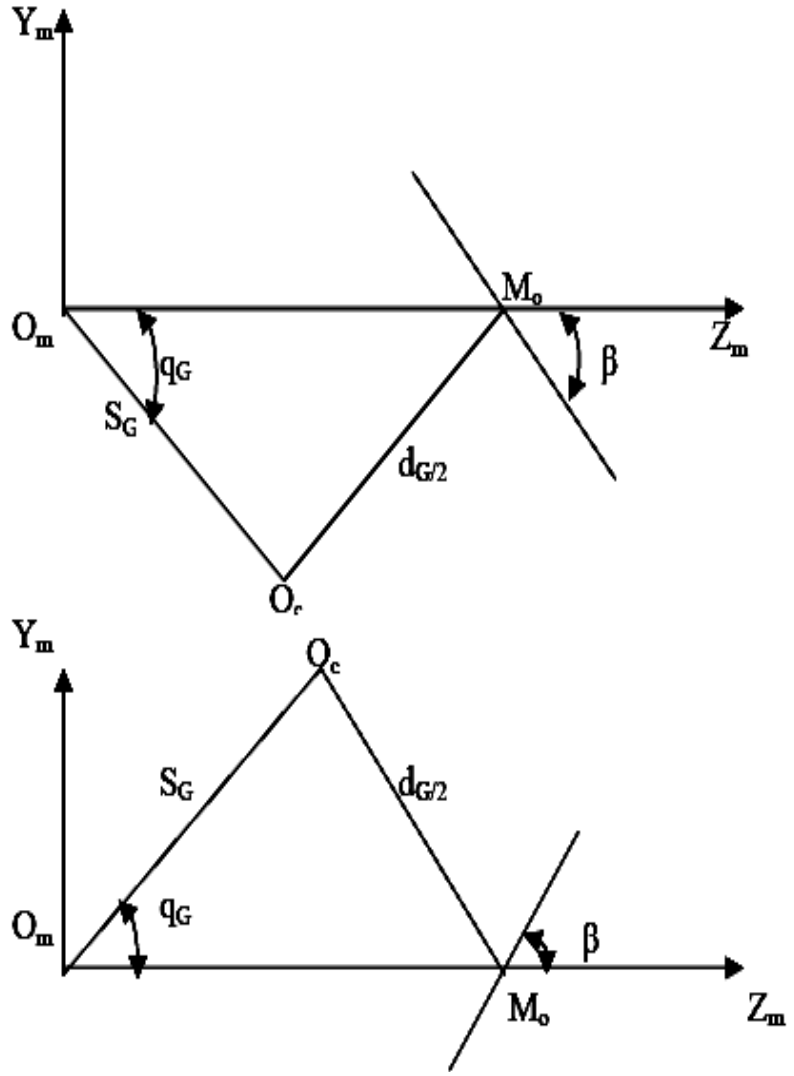

Fig.(5): The Front View Of The Installation Of The Head Cutter

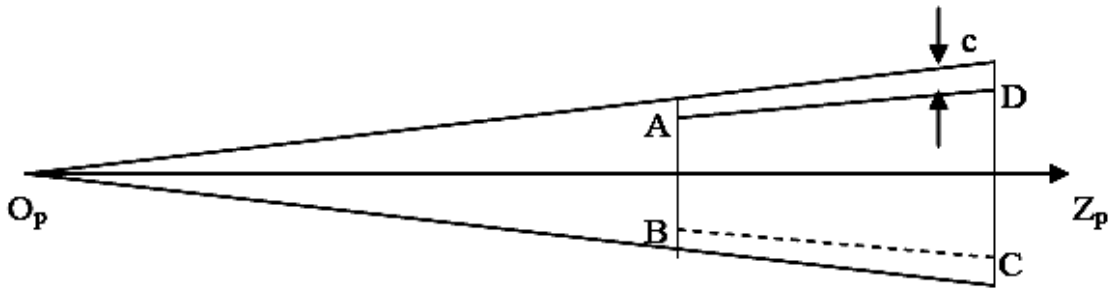

Fig. (6): Gear Tooth Surface

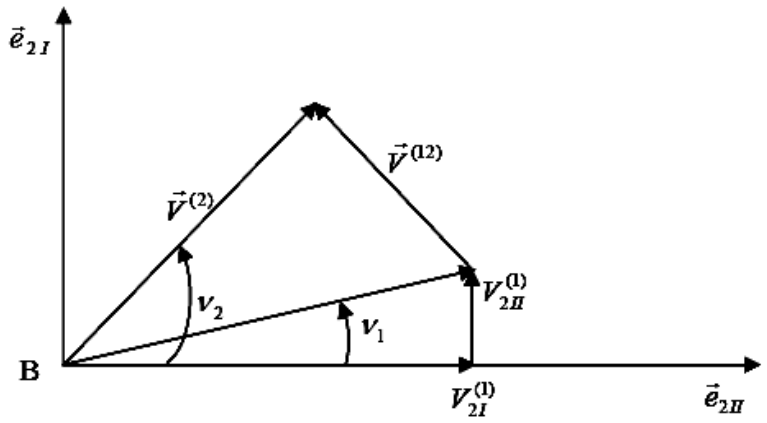

Fig.(7): Common Plane At The Mean Contact Point

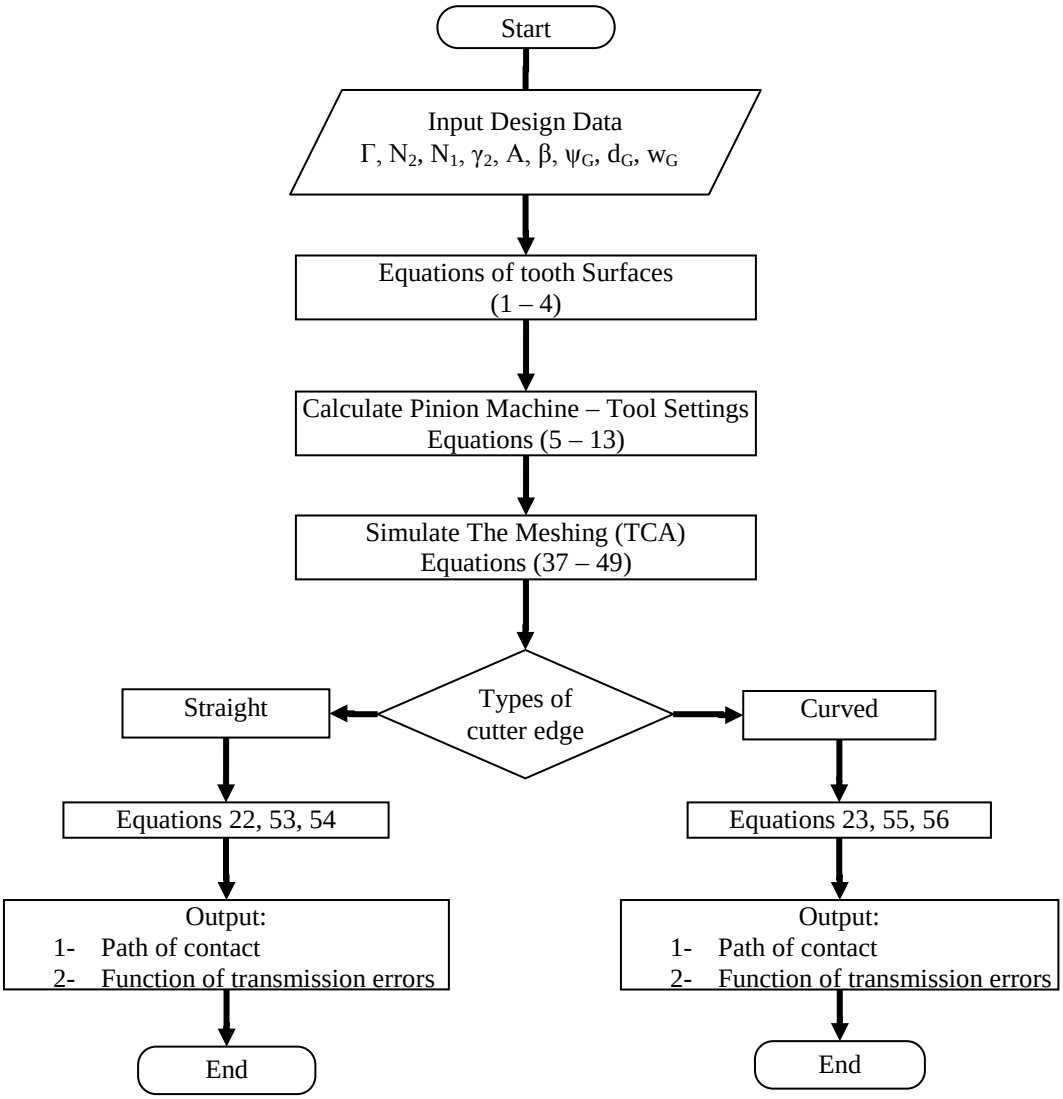

Fig.(8): Flow Chart Of Tooth Contact Analysis (TCA) Computer Program

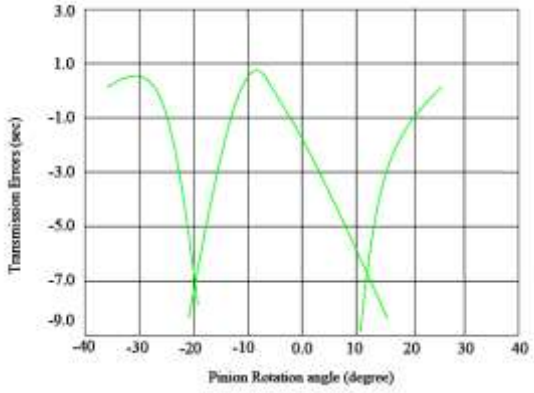

Fig.(9): TCA Output, Straight- Edged Blade, Alignment

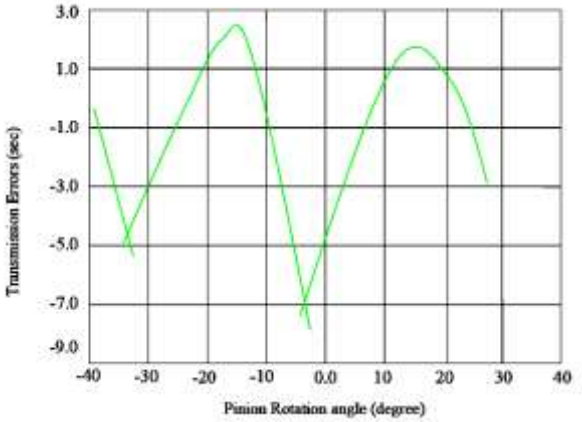

Fig.(10): TCA Output, Straight- Edged Blade, ΔA= +0.05 Mm

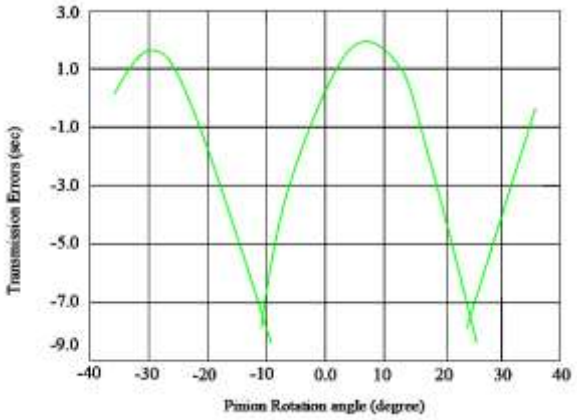

Fig.(11): TCA Output, Straight- Edged Blade, ΔA= -0.05 Mm

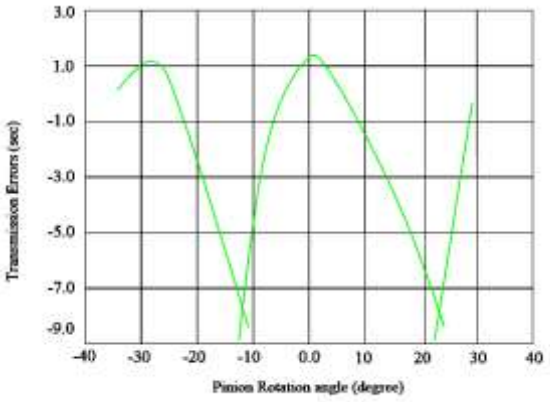

Fig.(12): TCA Output, Straight- Edged Blade, ΔV= +0.05 Mm

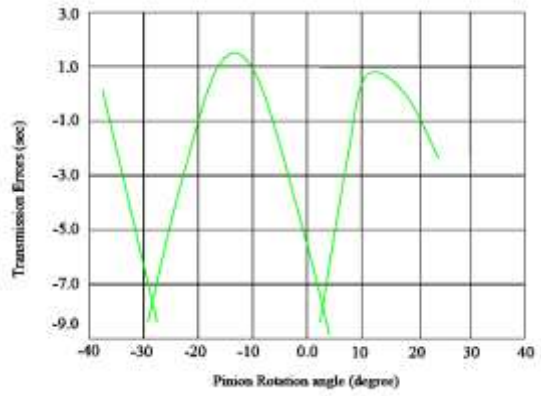

Fig.(13): TCA Output, Straight- Edged Blade, ΔV= -0.05 Mm

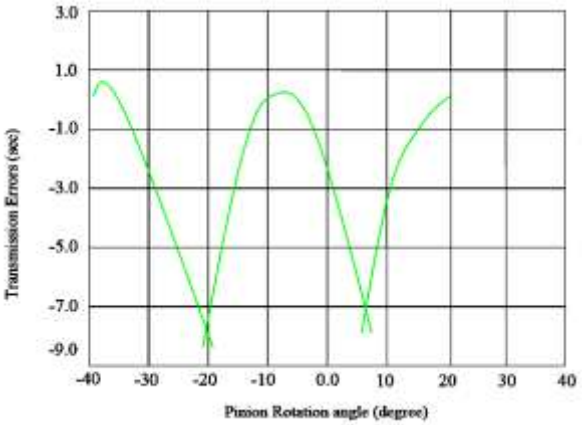

Fig.(14): TCA Output, Curved- Edged Blade, Alignment.

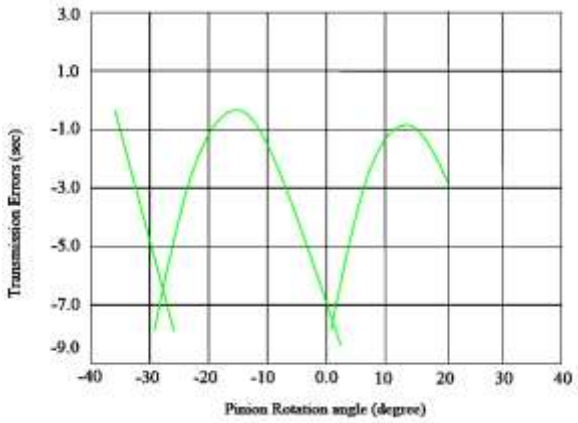

Fig.(15): TCA Output, Curved- Edged Blade, ΔA= +0.05

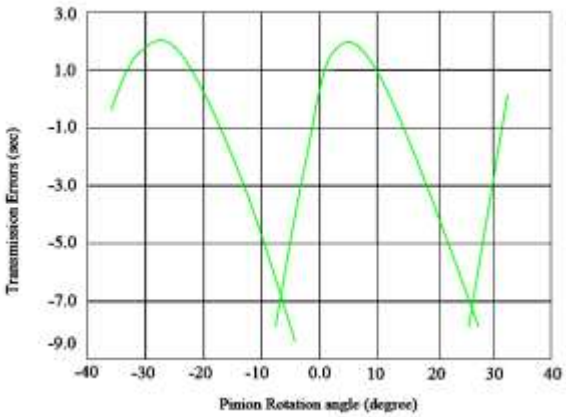

Fig.(16): TCA Output, Curved- Edged Blade, ΔA= -0.05

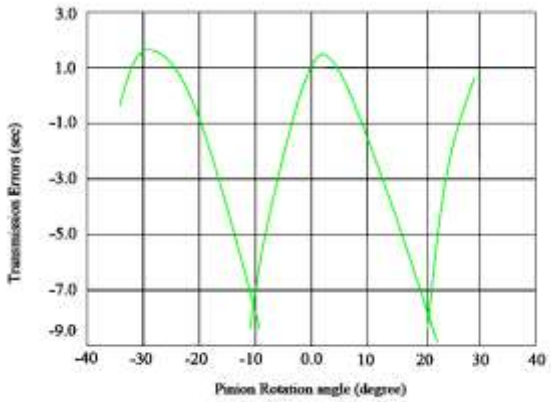

Fig.(17): TCA Output, Curved- Edged Blade, ΔV= +0.05

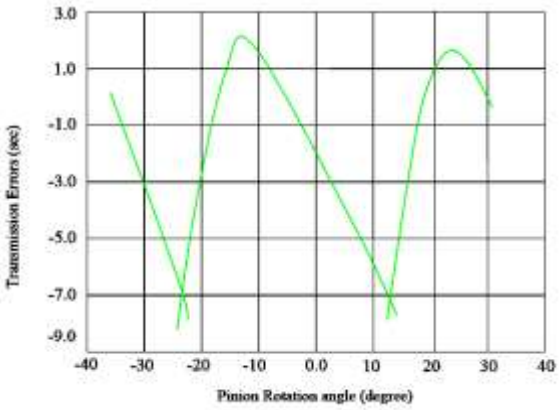

Fig.(18): TCA Output, Curved-Edged Blade, ΔV= -0.05

Table (1): Blank Data

	Pinion	Gear
Number of Teeth	10	41
Diametric Pitch	141.199 mm	
Shaft Angle	90^o	
Mean Cone Distance	81.940 mm	
Outer Cone Distance	96.418 mm	
Whole Depth	8.509 mm	
Working Depth	7.671 mm	
Clearance	0.838 mm	
Face Width	28.931 mm	
Root Cone Angle	12^o	72^o
Mean Spiral Angle	35^o	
Hand of Spiral	R.H	L.H

Table (2): Input Data

	Gear Convex Side	Gear Concave Side
Gear Blade Angle	20^o	
Gear Cutter Average Diameter	152.399 mm	
Gear Cutter Point Width	2.032 mm	
First Derivative of Gear Ratio	- 0.0037	0.0055
Semi major Axis of Contact Ellipse	4.343 mm	4.343 mm
Contact Path Direction Angle	90^o	75^o
Radius of Blade	1016 mm	1270 mm

Table (3): Pinion Mation Settings With Straight Blade

	Pinion Concave Side	Pinion Convex Side
Blade Angle	16.5561^o	22.9907^o
Tip Radius of Cutter	75.303 mm	77.987 mm
Radial	76.030 mm	68.525 mm
Cradle Angle	63.1869^o	54.1910^o
Ratio of Roll	0.229	0.25348
Machining Offset	4.421 mm	- 6.213 mm
Machine Center to Back + Sliding Base	0.539 mm	1.324 mm

Table (4): Pinion Mation Settings With Curved Blade

	Pinion Concave Side	Pinion Convex Side
Blade Angle	16.5561^o	22.9907^o
Blade Center	(293.548, 0, -896.849) mm	(499.998, 0, 1244.752) mm
Tip Radius of Cutter	75.811 mm	77.314 mm
Radial	75.077 mm	69.662 mm
Cradle Angle	63.0025^o	54.09^o
Ratio of Roll	0.23157	0.24915
Machining Offset	3.059 mm	-4.782 mm
Machine Center to Back + Sliding Base	0.429 mm	0.916 mm

REFERENCES

Faydor L. Litvin and Alfonso Fuentes (Computerized design, Generation, Simulation of meshing and contact, and stress analysis of formate cut spiral bevel gear drives), NASA CR-525, 2003

Faydor L. Litvin and Alfonso Fuentes (Gear geometry and applied theory), Second Edition, Cambridge University Press 2004

Gosselin C, Cloutier L and Brousseau J. (Tooth contact analysis of high conformity spiral bevel gear), NASA CR-341, 1991

Joseph L. Arvin and Thomas C. (Spiral bevel gear development, eliminating trial and error with computer technology), Gear Technology, The Journal of gear manufacturing, February 2003

Lelkes M. and Marialigeti J. (Cutting definition for kinematic optimization of spiral bevel gears), Hungary 2002.

Litvin F.L and Lee H.(Generation and tooth contact analysis of spiral bevel gears with predesigned parabolic functions of transmission errors), NASA TR-C-014, 1989

Litvin F.L, Q. Fan, A. Fuentes and R.F Handschuh (Computerized design, generation, simulation of meshing and contact of face-milled formate-cut spiral bevel gears), NASA TR-1224, 2001

Qi Fan (Kinematical simulation of face Hobbing indexing and tooth surface generation of spiral bevel and Hypoid gears), AGMA Technichal Paper 91 FTM, 2006

Robert F. Handschuh (Recent advances in the analysis of spiral bevel gears), NASA ARL-TR-1316, 1997

Theodore J. Krenzer (TCA of spiral bevel gears under load), Gleason work, 1981

NOMENCLATUTE

Index

C	tool surface (C = G, P)
W	work surface (W = 1, 2)
G	gear tool surface
P	pinion tool surface
1	pinion surface
2	gear surface
I	first principal
II	second principal

Matrices and Vectors

[A]	matrix represents the relation between the principal curvatures and directions for mating surfaces
[B]	matrix represents homogenous coordinates of point B
$[L_{ab}]$	matrix describes the transformation of vector from the S_b coordinate system to S_a coordinate system
$[M_{ab}]$	matrix describes the transformation of coordinates from the S_b coordinate system to S_a coordinate system
[N]	matrix represents components of normal vector $\vec{N}$
[n]	matrix represents components of unit normal vector $\vec{n}$
[ω]	matrix represents components of angular velocity vector $\vec{\omega}$
$\vec{B}$	Position vector of point B on a surface
$\vec{B}_u$	$\partial\vec{B}/\partial u$
$\vec{B}_v$	$\partial\vec{B}/\partial v$
$\vec{e}_I, \vec{e}_{II}$	Unit vectors along the principal directions of the surface at the contact point
$\vec{i}, \vec{j}, \vec{k}$	Base vectors along axes X, Y, and Z, respectively
$\vec{N}$	Normal vector of point B on a surface

$\vec{n}$	Unit normal vector of point B on a surface
$\vec{n}_u$	$\partial\vec{n}/\partial u$
$\vec{n}_v$	$\partial\vec{n}/\partial v$
$\vec{V}^{(CW)}$	Slide velocity of surfaces ∑C and ∑W
$\vec{V}$	Transfer velocity vector
$\vec{V}^{(1)},\vec{V}^{(2)}$	Velocity vectors of contact point in its motion over the pinion and gear surfaces, respectively
$\vec{\omega}$	Angular velocity vector
$\vec{\omega}^{(TQ)}$	Relative angular velocity vector of surface T with respect to surface Q
$\vec{\tau}$	Tangent vector

Latin Symbols

A	mean pitch cone distance, mm
A_0,A_1,A_2	Coefficient of a quadratic equation
B	Point on a surface
E_m	Machining offset, mm
L_m	Vector sum of machine center to back and sliding base
m_{G2}	Gear cutting ratio
$V_{2I}^{(1)},V_{2II}^{(1)}$	The projections of vector $\vec{V}^{(1)}$ on vectors $\vec{e}_{2I}$ and $\vec{e}_{2II}$, respectively, mm/sec
X_{MCB}	Machine center to back
X_{SB}	Sliding base, mm
W	Point width, mm
a	Constant
a_{ij}	Element of matrix [A]
b	Semi-minor axis of the contact ellipse, mm
c	Clearance, mm
d_g	Average diameter of gear cutter, mm
k_n	Normal curvature, mm
q	Cradle angle, deg
r	Tip radius of the cutter, mm
s	Radial setting, mm
t	Semi-major axis of the contact ellipse, mm

Greek Symbols

∑	Surface
Γ	Shaft angle, deg
α	Orientation angle of ellipse, deg
β	Mean spiral angle, deg
δ	Dedendum angle, deg
ϵ	Specified tolerance value
γ	Root angle, deg
μ	Pitch angle, deg
ϖ^{G2}	Angular velocity in relative motion, rad/sec
υ_1,υ_2	Angles formed between vectors $\vec{V}^{(1)}$ and $\vec{e}_{2I}$, and $\vec{V}^{(2)}$ and $\vec{e}_{2I}$, respectively, deg.